12-1-2016

Epigenetic Profiling Reveals a Developmental Decrease in Promoter Accessibility During Cortical Maturation in vivo

Ishwariya Venkatesh
Marquette University

Matthew T. Simpson
Marquette University

Denise M. Coley
Marquette University

Murray G. Blackmore
Marquette University, murray.blackmore@marquette.edu

Published version. *Neuroepigenetics,* Vol. 8 (December 2016): 19-26. DOI.

Neuroepigenetics 8 (2016) 19–26

Contents lists available at ScienceDirect

Neuroepigenetics

journal homepage: WWW.ELSEVIER.COM/LOCATE/NEPIG

Research paper

Epigenetic profiling reveals a developmental decrease in promoter accessibility during cortical maturation *in vivo*

Ishwariya Venkatesh *, Matthew T. Simpson, Denise M. Coley, Murray G. Blackmore

Department of Biomedical Sciences, Marquette University, 53201, USA

ARTICLE INFO

Article history:
Received 8 July 2016
Received in revised form 11 October 2016
Accepted 18 October 2016

ABSTRACT

Axon regeneration in adult central nervous system (CNS) is limited in part by a developmental decline in the ability of injured neurons to re-express needed regeneration associated genes (RAGs). Adult CNS neurons may lack appropriate pro-regenerative transcription factors, or may display chromatin structure that restricts transcriptional access to RAGs. Here we performed epigenetic profiling around the promoter regions of key RAGs, and found progressive restriction across a time course of cortical maturation. These data identify a potential intrinsic constraint to axon growth in adult CNS neurons. Neurite outgrowth from cultured postnatal cortical neurons, however, proved insensitive to treatments that improve axon growth in other cell types, including combinatorial overexpression of AP1 factors, overexpression of histone acetyltransferases, and pharmacological inhibitors of histone deacetylases. This insensitivity could be due to intermediate chromatin closure at the time of culture, and highlights important differences in cell culture models used to test potential pro-regenerative interventions.

1. Introduction

Axons in the mammalian central nervous system (CNS) possess low regenerative capacity, which limits functional recovery from CNS injuries. Although external inhibitory cues contribute to regenerative failure (Yiu and He, 2006; Case and Tessier-Lavigne, 2005), regeneration is also limited by an intrinsic inability of injured CNS neurons to reactivate transcriptional programs conducive to re-growth (Goldberg et al., 2002; Blackmore and Letourneau, 2006; Sun and He, 2010). Transcription factors are attractive targets to induce regenerative growth since they can simultaneously regulate the expression of multiple regeneration associated genes (RAGs). We and others have shown that forced expression of transcription factors (TFs) can result in regeneration of injured CNS neurons (Blackmore et al., 2012; Wang et al., 2015; Belin et al., 2015). However, this regenerative response is limited, highlighting the need to identify additional strategies to boost the efficacy of pro-regenerative TF treatments.

Two emerging concepts may explain the limited efficacy of over-expressing any single pro-regenerative transcription factor. First, appropriate combinations of TFs may be needed for maximal efficacy. For example, AP-1 factors JUN and ATF3 have been identified as hub TFs in transcriptional networks driving the peripheral nervous system (PNS) regeneration program, and dual expression results in elevated growth compared to either alone (Chandran et al., 2016; Fagoe et al., 2015; Li et al., 2015). Another emerging hypothesis is that the ability of TFs to activate needed target genes may be constrained at the level of chromatin structure around key RAGs in CNS neurons (Trakhtenberg and Goldberg, 2012). Chromatin modifications including methylation and acetylation of histone proteins represent well-established mechanisms to regulate gene expression (Bannister and Kouzarides, 2011). Acetylation, mediated by Histone Acetyltransferases (HATs) generally leads to a more relaxed, accessible chromatin state, whereas deacetylation mediated by Histone Deacetylases (HDACs) restricts DNA accessibility (Yang and Seto, 2007). Importantly, sensory neurons are known to relax chromatin around key RAGs as they mount successful regenerative responses to peripheral nerve injury (Puttagunta et al., 2014). Moreover, pharmacological inhibition of HDAC activity has been shown to enhance neurite outgrowth and RAG expression (Gaub et al., 2010; Finelli et al., 2013). Cortical neurons regenerate axons poorly after injury or stroke, and are known to undergo an age-dependent decline in regenerative ability during the early postnatal period (Bregman et al., 1989). Although existing data from other cell types suggest an important role for epigenetic regulation, chromatin structure and the phenotypic effects of histone modification remain uncharacterized in cortical neurons.

Here we explored the role of combinatorial AP-1 factor expression and epigenetic status in neurite outgrowth by postnatal cortical neurons, a

* Corresponding author at: Department of Biomedical Sciences, Marquette University, Milwaukee, WI 53201, USA.
E-mail address: ishwariya.venkatesh@marquette.edu (I. Venkatesh).

http://dx.doi.org/10.1016/j.nepig.2016.10.002

commonly used model for the study of molecular regulators of axon growth. First, pairwise combinatorial overexpression of AP-1 factors JUN, ATF3 and FOS revealed that although JUN overexpression produced expected increases in neurite length, combinatorial AP-1 expression produced no synergistic enhancement of outgrowth in this cell type. Next, profiling of the epigenetic landscape around promoter regions of key RAGs showed progressive chromatin restriction across a time course of cortical maturation. Early postnatal cortex showed intermediate restriction. Interestingly, in contrast to findings in other cell types, neurite outgrowth in neurons derived from early postnatal cortex was insensitive to HAT overexpression and HDAC inhibition (Puttagunta et al., 2014; Gaub et al., 2010). Overall the profiling data point toward developmental restriction of chromatin accessibility at regeneration-associated gene loci, identifying potential epigenetic constraints to axon growth in adult neurons. At the same time, the divergent neurite outgrowth data illustrate important differences across cell type in regards to the phenotypic impact of molecular interventions to enhance axon growth.

2. Methods

2.1. Cloning and plasmid preparation

To create constructs for screening and cell viability experiments, cDNA encoding JUN, ATF3 and FOS was prepared (QIAprep Spin Miniprep Kit, Qiagen 27106) from glycerol stocks of NIH Mammalian Genome Collection in pSPORT6-CMV expression vectors (Open Biosystems, ThermoFisher, Huntsville, Alabama) (Gerhard et al., 2004). To create nuclear-localized reporter constructs, the open reading frame of AP-1 factors (JUN aa1-334; ATF3 aa1-181; FOS aa1-380) was PCR-amplified and used to replace EBFP in expression vector CMV-EBFP-2A-H2B-EGFP as previously described (Simpson et al., 2015), creating CMV-JUN/ATF3/FOS-2A-H2B-EGFP. DNA was prepared by EndoFree Plasmid Maxi Kit (Qiagen 12362) and diluted to 1 μg/μl in endotoxin-free TE buffer.

2.2. Cortical culture, immunohistochemistry, and data analysis

All animal procedures were approved by the Marquette University Institutional Animal Care and Use Committee. Cortical neurons were prepared from Sprague Dawley rat pups (Harlan), and procedures for dissociation, transfection, and neurite outgrowth were performed as in (Simpson et al., 2015). Briefly, early postnatal (P3–P5) frontal cortices were dissected, and neurons dissociated. Cells were plated directly, or transfected then plated at a density of 10,000 cells/well into 24-well plates pre-coated with poly-D-lysine hydrobromide followed by laminin. Cells were maintained in culture for three days at 37 °C, 5% CO_2 in Enriched Neurobasal (ENB) media. For neurite outgrowth analysis, cultures were fixed with 4% PFA (Electron Microscopy Sciences 15710), and immunohistochemistry was performed for βIII-tubulin. Automated microscopy acquired images and neurites were traced using Cellomics Scan v6.4.0 (Thermo Scientific). Average total neurite length was quantified for greater than 100 cells per treatment. For AP-1 imaging, cells were left untransfected or transfected with CMV-JUN-2A-H2B-EGFP or CMV-ATF3-2A-H2B-EGFP and fixed after 3 days in culture. Immunohistochemistry was performed with DAPI nuclear stain and antibodies against c-Jun (Santa Cruz Biotechnology sc-1694) or ATF3 (Santa Cruz Biotechnology sc-188). Cellomics Cell Insight NXT (Thermo Scientific, Waltham, MA) acquired images for three channels: nuclear (DAPI), protein (JUN or ATF3), and reporter (EGFP). Compartmental analysis quantified object size and intensity for each channel and data were exported to Excel for analysis. Fragmented cells were eliminated from analysis based on DAPI size and intensity, and a transfection threshold was determined by comparing EGFP intensity to untransfected cells. Average JUN and ATF3 intensities were reported for $n > 250$ cells per treatment. For RAG IHC, P3–P5 cortical neurons were prepared as described above and fixed at 3 DIV. Immunohistochemistry was performed with DAPI nuclear stain and antibodies against GAP-43 (abcam ab16053, 1:500) or Galanin (Santa Cruz sc-25446, 1:500) and βIII-tubulin to identify neurons (Rb-Sigma T2200 (1:500), Ms Stem cell technologies 600100, 1:2000).

2.3. Pharmacological inhibition of HATs and HDACs

Cortical cultures were incubated for one day before addition of inhibitor drugs. HDAC inhibitor drugs Trichostatin A (TSA) (Santa Cruz Biotechnology sc-3511) and Scriptaid (Santa Cruz Biotechnology sc-202807) were constituted with DMSO into 1 mM and 5 mM stocks, respectively, and diluted to target concentrations in Hibernate E (Life Technologies A12476-01). HAT inhibitor drugs anacardic acid (Sigma A7236) and CPTH2 (Sigma C9873) were constituted into 20 mM stocks in DMSO and diluted to target concentrations in Hibernate E. Dilutions were done such that addition of 100 μl drug solution to the 500 μl ENB media in each well resulted in the testing concentration of 10 nM, 100 nM, 1 μM, 10 μM and 100 μM for HAT inhibitors and 5 nM, 10 nM, 50 nM, 100 nM and μM for HDAC inhibitors. Cultures were incubated one additional day before viability assays, or two days before neurite outgrowth analysis.

2.4. Cell viability assays

Viability assays were modified from Simpson et al. (2015). Neurons were transfected with EBFP-2A-mCherry or EBFP-2A-H2B-EGFP, plated at a density of 10,000 cells/well, and grown in culture for one day before addition of HAT and HDAC inhibitors, as described above. At 2DIV, media was removed and replaced with 0.01 μM Yo-Pro-1-Iodide (Cat# C3099, Life Technologies, Waltham, MA) or 0.15 μM propidium iodide (Cat# P1304MP, Molecular Probes, Eugene, OR), both in PBS containing 1 μg/ml Hoechst 33342 (Cat# H1399, Molecular Probes, Eugene, OR), and incubated at 37 °C for 30 min. Cellomics Cell Insight NXT (Thermo Scientific, Waltham, MA) acquired images for three channels: nuclear (Hoechst 33342), cell death stain (Yo-Pro-1-Iodide or propidium iodide), and reporter (EBFP-2A-mCherry or EBFP-2A-H2B-EGFP); compartmental analysis quantified intensities for each channel. Percent dead cells (Hoechst+/Yo-Pro-1-Iodide+ or Hoechst+/propidium iodide+) was quantified and subtracted from 100% to report number of live cells for greater than 1000 cells. Values from 2 to 3 biological replicates was averaged and analyzed using graphpad prism.

2.5. Quantitative chromatin immunoprecipitation

Motor cortices from female C57BL/6 mice (Harlan) were isolated at specified time points (Fig. 3). Freshly dissected cortices were incubated for 10 min at room temperature with gentle shaking in 1% formaldehyde solution (diluted from 16% PFA, Electron microscopy sciences, Hatfield, PA). The cross-linking reaction was quenched by the addition of glycine to a final concentration of 0.25 M. Cross-linked cells were washed 3 times in lithium chloride wash buffer (1.0% Igepal-CA630, 1.0% deoxycholate,1 mM EDTA,10 mM Tris-HCl (pH 8.1), 250 mM LiCl) followed by cell lysis in lysis buffer (10 mM Tris-HCl (pH 8.1), 10 mM NaCl, 1.5 mM $MgCl_2$, 0.5% Igepal-CA630, 5X Roche protease inhibitor (Cat# 04693132001)). Following lysis, cells were resuspended in nuclear lysis buffer (50 mM Tris-HCl (pH 8.1), 5 mM EDTA, 1% SDS, 5X protease inhibitor) and subjected to chromatin shearing through sonication to yield an average of 100–200 bp fragments. Samples were then incubated with 5 μg antibodies targeting specific histone modifications (H3K4me3 antibody – abcam ab8580, H3K4me27-ab6002) or non-specific IgG antibody (Cell signaling technology #2729) along with magnetic beads (Cat# 10001D, Thermofisher Scientific, Waltham, MA) overnight with gentle shaking at 4 degrees. Samples were then subjected to reversal of crosslinking, proteinase K digestion, and the recovered DNA was purified using Zymo ChIP DNA clean and concentrator (Cat# D5201, Zymo research Irvine, CA) and subjected to quantitative PCR.

2.6. Quantitative real time PCR analysis

Primers used in this study are listed in Supplementary Table 1. H3K4me3 marks are generally sharply enriched closest to the transcription start site, and H3K27me3 marks are acquired more broadly around the promoter and coding regions (Vastenhouw et al., 2010). Accordingly primer pairs were designed to span as closed to the transcription site as predicted by Promoter 2.0 software (Vastenhouw et al., 2010). To assess for relative changes in gene expression, quantitative PCR (qPCR) was performed on an ABI 7500 Fast Real time PCR system (Applied Biosystems, Carlsbad, CA) with SYBR green fluorescent label (Quanta Biosciences, Gaithersburg, MD). A dissociation step was performed at the end of the amplification phase to confirm a single, specific melting temperature for each primer set.

Cycle threshold values (Ct) for immunoprecipitated samples for each RAG was normalized to Ct values from chromatin not subjected to immunoprecipitation (input) that was diluted 1:100. Specific enrichment of histone marks to promoters was calculated by subtracting the noise determined by non-specific IgG and then normalized to diluted input. Normalized gene expression data from 3 biological replicates were averaged and depicted as fold change.

3. Results

3.1. AP-1 factors do not synergize to affect neurite outgrowth in postnatal cortical neurons

AP-1 factors are widely implicated in axon growth and known to work interactively to induce pro-regenerative transcriptional programs (Chandran et al., 2016; Fagoe et al., 2015; Raivich et al., 2004; Ruff et al., 2012; Makwana et al., 2010; Saijilafu et al., 2011; Fontana et al., 2012; Lerch et al., 2014; Seijffers et al., 2007; Campbell et al., 2005; Shokouhi et al., 2010; Saul et al., 2010; Hunt et al., 2012). Specifically, ATF3 and JUN show cooperative actions in regulating axon outgrowth in peripheral neurons (Chandran et al., 2016; Pearson et al., 2003; Nakagomi et al., 2003; Tsujino et al., 2000). Individual overexpression of JUN enhances neurite outgrowth in CNS neurons, but it is currently unknown whether other AP-1 factors may act synergistically with JUN in this cell type (Lerch et al., 2014).

We therefore adopted a well-established cell culture system to test co-expression of AP-1 factors JUN, ATF3 and FOS in assays of neurite outgrowth in post-natal CNS neurons (Simpson et al., 2015; Lerch et al., 2014; Blackmore et al., 2010; Moore et al., 2009). Post-natal cortical neurons were transfected in pairwise combinations with a base plasmid encoding one of the AP-1 factors (JUN, ATF3, FOS) or EBFP control along with test plasmids encoding JUN, ATF3, FOS, mCh negative control or DCLK1 positive control (Simpson et al., 2015; Blackmore et al., 2010). Transfected cells were identified by EGFP reporter expressed on base plasmid *via* a 2A peptide strategy, used previously for effective co-expression (Simpson et al., 2015; Blackmore et al., 2010; Tang et al., 2009). Plasmids were delivered at a ratio of 1 (base plasmid):4 (test plasmid), which results in over 90% co-transfection of both plasmids in EGFP + cells (Blackmore et al., 2010). Cells were plated on laminin substrates and maintained in culture for 3 days. Automated microscopy quantified neurite outgrowth from transfected neurons identified through βIII-tubulin immunostaining (Fig. 1C) and EGFP reporter (Fig. 1B). Each combinatorial gene treatment was tested in four independent experiments, and neurite lengths were normalized to mCherry control. As previously described (Simpson et al., 2015; Lerch et al., 2014; Blackmore et al., 2010), overexpression of test genes JUN and DCLK1 reliably increased neurite outgrowth (JUN-122.9% ± 5.74%, p-value < 0.05; DCLK1-143.9% ± 11.06%, p-value < 0.001, ANOVA with post-hoc Dunnett's) confirming assay sensitivity. Unlike JUN, neither ATF3 nor FOS overexpression increased neurite lengths. Moreover, no significant increases in neurite outgrowth above single JUN overexpression were observed in any of the combinatorial AP-1 factor gene treatments (Fig. 1E), including the JUN/ATF3 combination shown previously to produce synergistic gains in outgrowth from DRG neurons (Chandran et al., 2016). Immunohistochemistry confirmed robust overexpression of test genes including JUN and ATF3 in transfected neurons (Fig. 1F–O). In summary, these data indicate that forced co-expression of AP-1 factors shown to work co-operatively in peripheral neurons do not synergize to regulate neurite outgrowth in early cortical neurons.

3.2. Epigenetic profiling reveals developmental decrease in promoter accessibility in CNS neurons as they age in vivo

Besides potential TF/TF interactions, a second emerging concept in regeneration research is that axon growth may be constrained at the level of chromatin structure (Trakhtenberg and Goldberg, 2012; Puttagunta et al., 2014). Fundamentally, transcription of genes needed for regeneration depends not only on the presence of appropriate combinations of transcription factors (endogenous or supplied therapeutically), but also on chromatin structure that allows TF binding in key promoter regions (Trakhtenberg and Goldberg, 2012; Tedeschi, 2011). Chromatin accessibility can be predicted by enrichment for specific histone marks that are commonly associated with euchromatin (accessible chromatin) *vs* heterochromatin (restricted chromatin). Therefore, as a first step in linking regenerative ability to chromatin structure, we examined histone marks in cortical tissue across a developmental time-course that spans a period when CNS neurons are known to decline in regenerative ability (Bregman et al., 1989).

Six RAGs with well-established roles in mediating axon outgrowth and guidance were selected for initial analysis: *gap43*, *cap23*, *sprr1a*, *integrinα7*, *hsp27*, and *galanin* (Frey et al., 2000; Bonilla et al., 2002; Bomze et al., 2001; Zhang et al., 2005; Hobson et al., 2013; Eva and Fawcett, 2014; Williams et al., 2005; Ma and Willis, 2015). We first examined the histone modification H3K4me3, commonly associated with euchromatin/genomic loci undergoing active transcription, and H3K27me3, associated with heterochromatin/genomic loci not actively transcribed (Bannister and Kouzarides, 2011). H3K4me3 and H3K27me3 marks rarely co-exist around gene promoters and mostly presence of one modification excludes the presence of the other (Vastenhouw et al., 2010).

In initial validation experiments quantitative chromatin immunoprecipitation was used to assess the promoter regions of selected RAGs at E15, an age when these genes are actively transcribed (Ma and Willis, 2015). The promoter regions of constitutively expressed *gapdh* and non-expressed *Hoxc10*, with previously established methylation marks, served as controls. In E15 cortices, the H3K4me3 ("open") mark was enriched 15-fold around *gapdh* locus (p-value < 0.0001 compared to non-specific antibody, one-way ANOVA with post-hoc Dunnett's) but showed no enrichment at the *Hoxc10* locus, confirming antibody efficacy and assay sensitivity (Fig. 2B). H3K4me3 was also highly enriched at *sprr1a*, *integrinα7*, *galanin* and *gap43* loci, consistent with their embryonic expression (p-value < 0.0001,one-way ANOVA with post-hoc Dunnett's) (Fig. 2B). In contrast, *hsp27* and *cap23* gene loci showed no significant enrichment for the H3K4me3 mark (Fig. 2B). The H3K27me3 "closed" mark was enriched 14-fold around the *Hoxc10* gene locus (p-value < 0.0001, one-way ANOVA with post-hoc Dunnett's) but was not significantly enriched at the *gapdh* locus, again confirming the expected antibody behavior (Fig. 2C). Consistent with high embryonic expression, none of the RAG gene loci showed enrichment for the H3K27me3 mark (Fig. 2C). These experiments confirm that the chosen histone marks H3K4me3 and H3K27me3 reliably correlate with euchromatin/heterochromatin in four of the six gene loci examined in E15 cortices, and can be used to detect chromatin accessibility around these loci. Promoters for *hsp27* and *cap23* do not show enrichment with either histone mark, suggesting that other histone modifications may be associated with these gene loci. Further analyses were restricted only

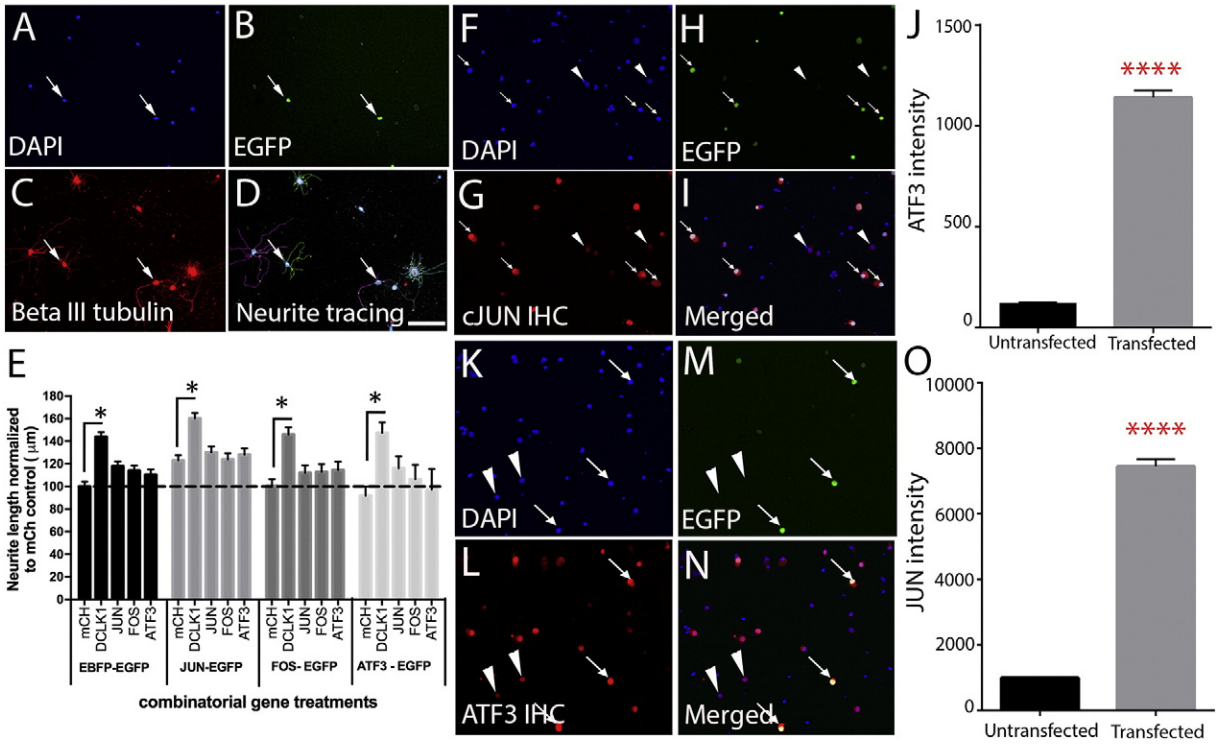

Fig. 1. JUN mediated enhancement of neurite outgrowth is not increased by AP-1 factor co-expression. P3 cortical neurons were co-transfected with plasmid DNA and cultured on laminin substrates for 3 days. (A–D) Images were acquired through automated microscopy (Nuclear: DAPI, Neuronal: βIII-tubulin, Transfection: EGFP). Cells positive for neuron-specific βIII-tubulin and EGFP (arrows, B and C) were used for subsequent analyses. (E) Bars show the average neurite length in cells expressing combinations of AP-1 transcription factors normalized to mCherry control. Test genes included DCLK1 and JUN, both of which showed expected changes in neurite length, confirming assay sensitivity. *p-Value < .05 ANOVA with post-hoc Dunnett's, N > 100 cells in three replicate experiments, error bars represent SEM, F-value-1.32. Scale bar is 50 μm. (F–O) P3 cortical neurons were transfected with ATF3-EGFP (F–I) or JUN-EGFP (K–O) reporter plasmids and cultured on laminin substrates for 3 days. Cells were then stained with antibodies targeting ATF3/JUN followed by automated compartmental analysis to compare ATF3/JUN intensities in untransfected cells *vs* transfected cells within the same well. J,O - Bars show average ATF3 (J) or JUN (O) fluorescence intensities in untransfected cells and cells transfected with plasmids to overexpress ATF3 or JUN. ****p-Value < 0.0001 unpaired *t*-test, N > 1000 cells, error bars represent SEM.

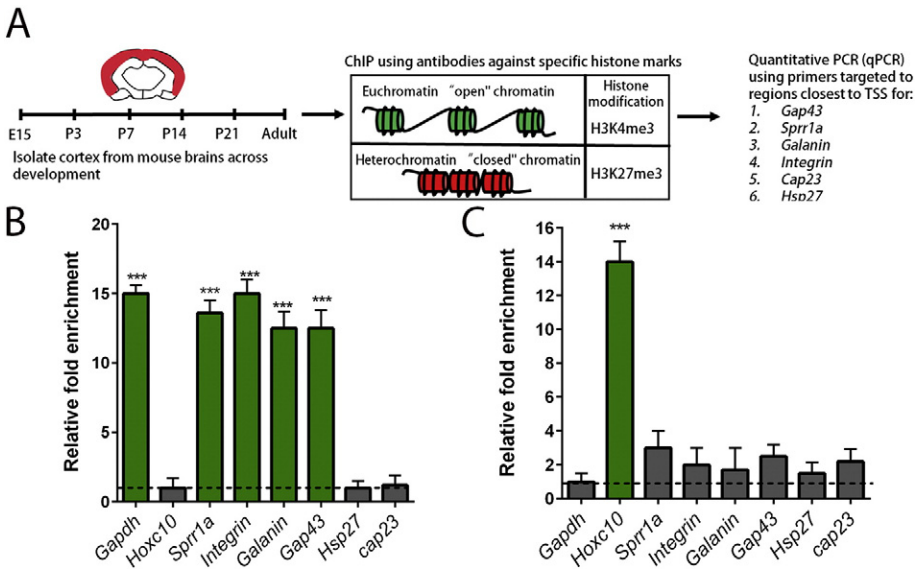

Fig. 2. Genomic loci corresponding to regeneration associated genes are associated with open chromatin during development. RAG promoter sequences were enriched by ChIP in E15 cortex using antibodies targeted to open and closed chromatin marks. Specific enrichment of histone marks to promoters is calculated by subtracting the noise determined by non-specific IgG and then normalized to diluted input. Dotted line represents relative fold enrichment observed in non-specific IgG control (A) Experimental schematic outlining the epigenetic profiling experiment across age as CNS neurons mature *in vivo* (B) Significant fold enrichment over non-specific background is observed in 4 of the RAG promoter sequences for the H3K4me3 (open chromatin) histone mark, comparable to positive control *gapdh* locus (p-value < 0.0001, one-way ANOVA with post-hoc). No significant enrichment over background is observed in *Hoxc10* (neg ctrl), *hsp27* or *cap23* loci. (C) No significant enrichment over non-specific background is observed for H3K27me3 mark in any of the RAG loci profiled. *Hoxc10* (p-value < 0.001, one-way ANOVA with post-hoc) and *gapdh* loci serve as positive and negative controls for the H3K27me3 modification, confirming antibody specificity. Error bars represent SEM. N = 2–3 biological replicates.

to the four RAGs that showed significant enrichment for H3K4me3 mark in E15 cortices.

We then investigated changes in chromatin state around promoters of the selected RAGs over a time series of cortical maturation *in vivo* (E15, P3, P7, P14, P21, and adult). When examining the H3K4me3 open chromatin mark, the *gapdh* locus displayed ~15-fold enrichment at all ages, consistent with its continual expression. In contrast, the *sprr1a*, *integrinα7*, *galanin* and *gap43* loci showed a ~2-fold decrease (p-value < 0.001, two-way ANOVA with post-hoc Dunnett's) between E15 and P7, followed by a gradual decline, to levels in adulthood there were not significantly higher than background signal (Fig. 3). The H3K27me3 "closed" mark was highly enriched at the *Hoxc10*, but not *gapdh*, at all ages (Fig. 4). All four RAGs displayed a significant increase in enrichment for H3K27me3 with age, with ~15-fold increase in the adult cortex compared to embryonic (p-value < 0.00001, two-way ANOVA with post-hoc Dunnett's). Interestingly, there were differences in the timing of this transition among the RAGs, with some RAGs showing enrichment for closed chromatin mark as early as P3 (*sprr1a*), and others gaining enrichment at P7 (*gap43*), P21 (*integrinα7*) and only in adult cortex (*galanin*) (Fig. 4). Overall these experiments demonstrate increase in restricted chromatin around promoters of key RAGs as CNS neurons mature *in vivo*, identifying a potential constraint limiting the intrinsic regenerative capacity of CNS neurons.

3.3. Global manipulation of HDAC/HAT activity does not enhance neurite outgrowth in post-natal CNS neurons

Chromatin accessibility is gated by acetylation of histones, modulated by the opposing actions of Histone Acetyltransferases (HATs) and Histone Deacetylases (HDACs) (Lee and Workman, 2007). HAT-mediated acetylation of histones generally leads to a more relaxed, accessible chromatin state, whereas HDAC-mediated deacetylation restricts DNA accessibility. Overexpression of HATs and/or

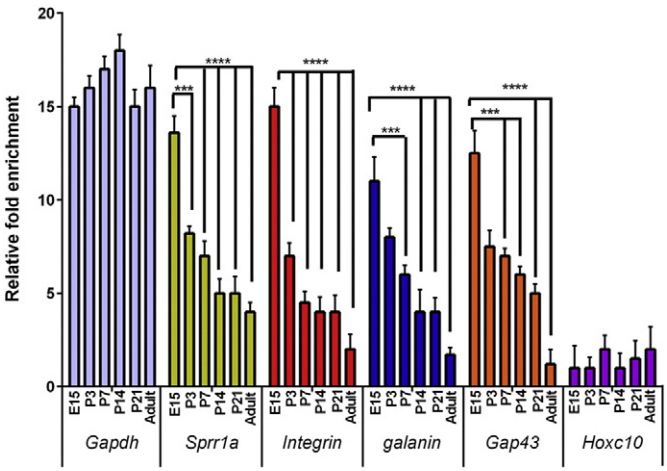

Fig. 3. Promoter regions of RAGs show reduced enrichment for open chromatin as CNS neurons mature *in vivo*. RAG promoter sequences were enriched by ChIP in cortices across age using antibodies targeted to euchromatin mark- H3K4me3. Specific enrichment of histone marks to promoters is calculated by subtracting the noise determined by non-specific IgG and then normalized to diluted input. *Gapdh* gene locus shows significant enrichment for H3K4me3 mark across all ages, confirming antibody efficacy and specificity. Significant fold enrichment for H3K4me3 is observed in E15 cortex across all genes comparable to *gapdh* positive control locus (p-value < 0.0001, one-way ANOVA with post-hoc Dunnett's). For 2 of the RAGs - *sprr1a* and *integrinα7*, there was a significant reduction in enrichment of H3K4me3 mark between E15 and P3 (p-value < 0.01, two-way ANOVA with post-hoc Dunnett's), with most all genes showing significant reduction in enrichment for open chromatin between E15 and P7(***p-value < 0.001, two-way ANOVA with post-hoc Dunnett's), with the most significant reduction in enrichment observed between E15 and P14 - adult cortex (p-value < 0.0001, two-way ANOVA with post-hoc Dunnett's). F-value-207.7, error bars represent SEM. N = 2–3 biological replicates.

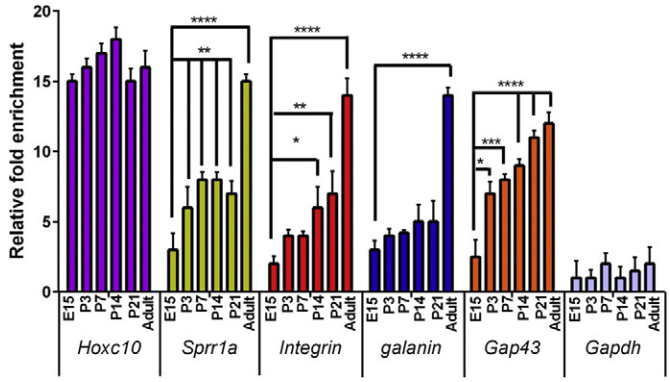

Fig. 4. Promoter regions of RAGs associated with heterochromatin in the adult cortex RAG promoter sequences were enriched by ChIP in cortices across age using antibodies targeted to heterochromatin mark - H3K4me27. Specific enrichment of histone marks to promoters was calculated by subtracting the noise determined by non-specific IgG and then normalized to diluted input. *Hoxc10* gene locus shows significant enrichment for H3K27me3 mark across all ages, confirming antibody efficacy and specificity. Enrichment for closed chromatin mark is not significant over background at E15 for any of the RAGs. Gene loci gain enrichment for closed chromatin mark as neurons age, with the most significant fold enrichment for H3K4me27 mark observed in adult cortex. Levels of H3K27me3 enrichment in adult cortex for all genes are comparable to *Hoxc10* positive control locus (p-value < 0.0001, one-way ANOVA with post-hoc Dunnett's). F-value-169. Error bars represent SEM. N = 2–3 biological replicates.

inhibition of HDAC activity, both predicted to lead to a more relaxed chromatin state, have been shown to promote increased RAG transcription and axon regeneration in sensory neurons (Puttagunta et al., 2014; Finelli et al., 2013; Lv et al., 2012; Lv et al., 2011). Early postnatal cortical neurons are widely used as a tractable model for the study of the molecular control of axon growth (Simpson et al., 2015; Lerch et al., 2014; Blackmore et al., 2010; Zou et al., 2015), but it is currently unknown how they might respond to global manipulation of HAT or HDAC activity.

We first tested forced expression of two well-studied HATs, or KAT2B (PCAF), in post-natal cortical neurons. All constructs expressed an EGFP reporter *via* 2A peptide, and were co-expressed with either mCherry or DCLK1 as a positive control for growth promotion. Cells were maintained in culture for 3 days, then fixed and subjected to automated tracing of neurite length as described above. As expected, DCLK1 expression robustly increased neurite length compared to EBFP control (EBFP + DCLK1-143.9% ± 11.06%, p-value < 0.001, One-way ANOVA with post-hoc Dunnett's). In contrast, KAT2A and KAT2B expression had no effect on neurite length, either in basal conditions or when combined with DCLK1 (Fig. 5A). Thus, forced over-expression of HATs-KAT2A/KAT2B does not promote increased neurite outgrowth in early CNS neurons. This is in contrast to what is observed in the PNS, wherein overexpression of KAT2B alone was sufficient to promote axon outgrowth to levels comparable to the well-studied conditioned-lesion paradigm (Puttagunta et al., 2014).

We next tested pharmacological manipulation of HDAC and HAT activity. First, broad-spectrum HDAC inhibitors TSA and Scriptaid were applied to post-natal cortical neurons in concentrations between 5 and 50 nM, previously shown to increase neurite outgrowth in other neuronal cell types (Gaub et al., 2010; Finelli et al., 2013). HDAC inhibitors at these concentrations are not expected to affect cell survival (Gaub et al., 2010), and indeed viability assays showed no effects at concentrations below 100 nM (Fig. S1). Cells were subjected to automated neurite tracing two days post-inhibitor treatment, with neurite lengths normalized to untreated cells. Interestingly, we did not observe any enhancement in neurite outgrowth at any concentration of HDAC inhibitors (Fig. 5B). In complementary experiments, broad-spectrum inhibitors of HAT activity were also tested, to evaluate effects of blocking HAT activity on net neurite outgrowth. Anacardic acid (AA) and CPTH2 were applied to post-natal cortical neurons in

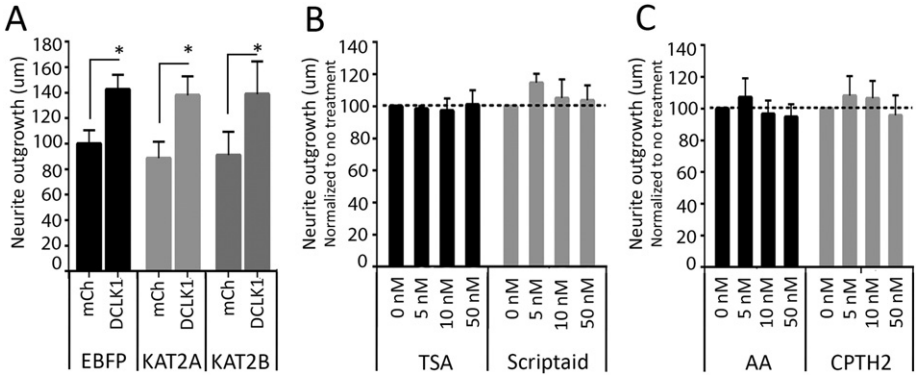

Fig. 5. Global manipulation of HAT/HDAC activity does not enhance neurite outgrowth in post-natal cortical neurons. (A) P3 cortical neurons were co-transfected with plasmids to overexpress HATs (KAT2A, KAT2B) or control plasmids (EBFP), along with mCh negative control and DCLK1 and cultured on laminin substrates for 3 days. Images were acquired through automated microscopy and tracing quantified neurite length. Bars show the average neurite length in cells overexpressing HATs normalized to mCherry control. mCh and DCLK1 controls showed expected changes in neurite length in both HAT combinations, confirming assay sensitivity. (B) P3 cortical neurons were cultured on laminin substrates and Class I and II HDAC pharmacological inhibitors Trichostatin A (TSA) and Scriptaid were added 1DIV in increasing concentrations (0,5,10,50 nM) and allowed to incubate for 2 days before automated neurite outgrowth analysis. Bars show the average neurite length in cells treated with HDAC inhibitors normalized to no treatment (C) P3 cortical neurons were cultured on laminin substrates and Class I and II HAT pharmacological inhibitors Anarcardic acid (AA) and CPTH2 were added 1DIV in increasing concentrations (0,5,10,50 nM) and allowed to incubate for 2 days before automated neurite outgrowth analysis. Bars show the average neurite length in cells treated with HAT inhibitors and normalized to no treatment. For all experiments, n > 100 cells (three biological replicates), error bars represent SEM.

increasing concentrations as previously described (Lin et al., 2015). Again, automated analysis of neurite lengths detected no significant effect on neurite outgrowth at any of the concentrations tested (Fig. 5C). Cell viability assays confirmed no effects on cell survival at the tested concentrations (Fig. S1). Thus postnatal cortical neurons, derived from an age at which chromatin marks indicate intermediate accessibility at key RAGs, appear to display neurite outgrowth that is insensitive to global pharmacological inhibitors of HDAC and HAT activity.

4. Discussion

Here we examined chromatin modifications in the maturing cortex and evaluated two emerging strategies to promote neurite outgrowth in cultured cortical neurons. In contrast to previous reports in other cell types, we found that neither combinatorial overexpression of AP-1 factors nor treatments that target histone acetylation affected neurite outgrowth in this assay system. At the same time we detected progressive chromatin restriction around promoters of crucial RAGs as the cortex matures *in vivo*, and found chromatin restriction to be in an intermediate state at the early postnatal period. Thus, in the adult, chromatin restriction may represent an intrinsic constraint that could limit the regenerative capacity of CNS neurons, highlighting the need to optimize targeted genetic/epigenetic combinatorial manipulations to boost the intrinsic capacity of CNS neurons. On the other hand, although postnatal CNS neurons are widely used as a model to investigate the molecular control of axon growth, their capacity for neurite extension appears to be insensitive to commonly used strategies to alter acetylation.

4.1. Combinatorial TF treatments – differential requirements in CNS vs PNS

Identifying optimal TF/TF combinations is an important research goal in regenerative research. Although we and others have shown that forced expression of single pro-regenerative TFs can act to enhance axon regeneration in injured CNS neurons (Blackmore et al., 2012; Wang et al., 2015; Belin et al., 2015), it is increasingly clear that combinatorial TF treatments are more effective than single TF treatments (Belin et al., 2015; Sun et al., 2011; Jin et al., 2015). Indeed, *in silico* analyses of peripheral neurons indicates that multi-nodal transcriptional networks, rather than isolated activities by individual TFs, drives regenerative axon growth (Chandran et al., 2016; Li et al., 2015; Tedeschi, 2011; van Kesteren et al., 2011; Geeven et al., 2011; Michaelevski et al., 2010). AP-1 factors JUN and ATF3 are classic regeneration-associated TFs, likely involved in coordinating the peripheral nerve regeneration program based on their expression patterns in transcriptional profiling datasets (Blackmore, 2012). Forced over-expression of JUN enhances neurite outgrowth in post-natal cortical neurons (Lerch et al., 2014) and constitutive overexpression of ATF3 is known to enhance peripheral nerve regeneration (Seijffers et al., 2007). Since these factors are predicted to work cooperatively to drive RAG gene expression in injured neurons (Pearson et al., 2003; Nakagomi et al., 2003; Tsujino et al., 2000), there is a strong possibility of synergy in regulating neurite outgrowth. Indeed, in a recent study in cultured peripheral neurons, ATF3/JUN combinations promoted neurite outgrowth to a greater extent than either factor alone (Chandran et al., 2016).

Thus it is somewhat unexpected that in postnatal cortical neurons, pairwise overexpression of JUN, ATF3, or FOS did not lead to further increases in neurite outgrowth above JUN alone (Fig. 1). What could explain this lack of synergy? It is possible that AP-1 factors show functional redundancy in activating downstream RAGs in early post-natal CNS neurons. A second possibility is that AP-1 factors may function in a cell-type specific manner to promote growth, depending on the availability of molecular components that may interact with or modify JUN/ATF3 to render them functional. For instance JNKs are activated in response to stress/axotomy and are required to activate JUN and ATF3 and such upstream regulators may be naturally available in a DRG cellular context, but missing in CNS neurons limiting full efficacy of these factors (Coffey, 2014). Lastly, it is possible that the stoichiometry of the co-expressed factors, which is not well controlled in this overexpression paradigm, may favor the formation of homo- or heterodimers that interfere with pro-regenerative function. AP-1 factors are known to form both homo- and heterodimers that differ greatly in transcriptional activity, and in some cases AP-1 homodimer formation can even lead to hampered/repressed target gene expression (Nakagomi et al., 2003; Hai and Hartman, 2001). Thus it is possible that an optimal ratio of JUN/ATF3 expression is needed for efficient axon growth, but was not achieved by the plasmid co-transfection strategy used in this study. These possibilities highlight the complexity in successfully recapitulating PNS regeneration specific transcriptional networks in a CNS context, and identify important factors to take into

account when designing efficient combinatorial gene treatments in CNS neurons.

4.2. Epigenetic manipulation of axon growth

Our data also offer circumstantial support for the emerging hypothesis that a major barrier to initiating a pro-growth genetic program in CNS neurons exists at the level of the DNA, that is, at the level of chromatin structure. It is well established that many CNS neurons, including those in the cortex, decline in their intrinsic regenerative ability during postnatal development (Goldberg et al., 2002; Bregman et al., 1989; Moore et al., 2009; Chen et al., 1995; Dusart et al., 1997). A central feature of this reduced regenerative ability is the developmental reduction in expression of key RAGs (Karimi-Abdolrezaee et al., 2002), and a frequent failure to re-express those RAGs after axotomy (Plunet et al., 2002; Mason et al., 2003). The current data show pronounced changes in histone marks in RAG promoter regions, indicative of progressive chromatin closure during postnatal development. For atleast one RAG, GAP-43, the acquisition of "closed" chromatin marks correlate well with observed mRNA expression patterns across age in corticospinal motor neurons (Karimi-Abdolrezaee et al., 2002). A major caveat to this finding regards the use of whole cortical tissue, as opposed to purified neurons. It is possible that chromatin changes in non-neural cells and/or developmental shifts in the cellular composition of the cortex could contribute to the observed changes. Given the high neuronal proportion in the overall cortical cell population, however, it is quite unlikely that the magnitude of the near-complete reversal of the H3K4me3 and H3K27me3 marks with age can be explained entirely by shifts in non-neuronal cells. This is especially true considering the known neural-specific expression of these RAGs (Ma and Willis, 2015). The purification of neurons from mature cortex is quite challenging and outside the technical scope of this manuscript. Thus, although definitive conclusions must await the analysis of purified neurons, the current data provide a very strong indication that chromatin structure at genes involved in regenerative axon growth undergoes profound restriction as neurons age.

To test the emerging link between chromatin structure and axon growth, previous studies have genetically or pharmacologically manipulated chromatin accessibility in functional assays of axon growth. Genes that are not actively transcribed, such as RAGs in non-regenerating CNS neurons, may be held in a "closed" chromatin state, rendering them inaccessible to transcription factors (Trakhtenberg and Goldberg, 2012). One of the best-characterized and readily manipulated epigenetic modifications is acetylation of histones, mediated by Histone Acetyltransferases (HATs) and Histone Deacetylases (HDACs). In the simplest model, acetylation mediated by HATs leads to a more relaxed chromatin state with increased accessibility to DNA-binding regions and deacetylation mediated by HDACs leads to a restricted chromatin state, blocking DNA accessibility (Yang and Seto, 2007; Cho and Cavalli, 2014). Consistent with this, experiments in cerebellar granular neurons found that manipulation of HDAC/HAT enzyme activity to favor open relaxed chromatin enhanced RAG transcription and also modestly improved neurite outgrowth (Gaub et al., 2010). Also, studies have shown that inhibition of HDAC activity results in increased RAG gene transcription, peripheral nerve outgrowth and improved behavior in mice challenged with spinal injuries (Finelli et al., 2013; Lv et al., 2012; Lv et al., 2011; Lee et al., 2012). Furthermore, in regeneration-competent neurons, axonal injury triggers relaxation of chromatin at key loci corresponding to crucial RAGs (Puttagunta et al., 2014). However, we find that overexpression of HATs-KAT2A and KAT2B/pharmacological inhibition of Class I or II HDAC activities in early post-natal cortical neurons does not lead to significant enhancement in neurite outgrowth.

What could explain the lack of effects upon manipulation of HDAC/HAT activity in early post-natal CNS neurons? First, our epigenetic profiling experiments indicate that in the early postnatal cortex, RAG promoters show decreased accessibility compared to embryonic immature neurons, but the restriction is not as severe as what is observed in adult neurons. It could be that in neurons prepared at this age, chromatin structure around key RAG promoters does not yet limit access, negating the need for additional treatments to relax chromatin. This is especially relevant because chromatin restriction genome-wide has been shown to proceed at a slower pace when cells are maintained *in vitro*, than what is observed in an *in vivo* environment (Frank et al., 2015). Consistent with this, we observe clear RAG expression for GAP-43, Galanin in early post-natal neurons maintained *in vitro* (Fig. S2), same age as the cells used in the HDAC/HATi experiments. The use of fully adult CNS neurons in cell culture models of axon growth is largely prevented by poor viability, and therefore embryonic or early postnatal cells are typically used. Hence although post-natal cortical neurons have proven to be a highly effective model in which to identify genes important for axon growth (Simpson et al., 2015; Blackmore et al., 2010), older neurons maintained in culture may be more suited for epigenetic screening studies.

Another possibility for lack of effects upon broad manipulation of HDAC/HAT activity involves non-specificity. It is well known that chromatin remodeling complexes and histone-modifying enzymes act widely across the eukaryotic genome (Langst and Manelyte, 2015; Nemeth and Langst, 2004). Although engaging HATs and HDACs to alter chromatin structure is an obvious approach to relieve epigenetic constraints, non-specific effects of global overexpression/inhibition must be considered. In line with this, research in cell re-programming and nervous system development has revealed that it is not the absolute expression levels of HATs/HDACs, but rather how these chromatin remodelers are directed to relevant genomic loci that determines successful downstream gene transcription *via* targeted chromatin remodeling (Frank et al., 2015; Koche et al., 2011). In addition, non-histone targets of HATs and HDACs must also be considered. For example, HATs are also known to target microtubules in the axoplasm. Thus, although HAT inhibition might be expected to close chromatin and thereby restrict axon growth, in fact HAT inhibition can increase neurite outgrowth in DRG neurons, a finding that may be explained by microtubule stabilization (Lin and Smith, 2015). Thus a major and unmet challenge regarding epigenetic modulation may be the need to develop more precise targeting strategies, such that relevant chromatin remodelers are directed to the precise genomic loci for targeted chromatin remodeling.

Overall we report findings that hint at potential strategies going forward to boost intrinsic regenerative capacity in CNS neurons (Yiu and He, 2006). Early developmental genetic interventions may be more successful in triggering pro-regenerative gene cascades, since adult neurons display constricted chromatin around key RAG promoters (Case and Tessier-Lavigne, 2005). Combining targeted chromatin remodeling with pro-regenerative TFs may be necessary to allow full efficacy of transcription factor treatments (Goldberg et al., 2002). Although combinatorial transcription factor treatments are likely better than individual treatments, the lack of AP-1 synergy in the present experiments highlight differences across cell type in the potential efficacy of identified transcriptional modules.

Supplementary data to this article can be found online at doi:10.1016/j.nepig.2016.10.002.

Conflict of interest

None.

Acknowledgments

This work was supported by grants from NINDS (1R21NS095276-01) and the Bryon Riesch Paralysis Foundation (02650-74861(2015)).

This work was also supported by Craig.H.Nielsen foundation (post-doctoral fellowship).

References

Bannister, A.J., Kouzarides, T., 2011. Cell Res. 21, 381 (Mar).
Belin, S., et al., 2015. Neuron 86, 1000 (May 20).
Blackmore, M.G., 2012. Int. Rev. Neurobiol. 105, 39.
Blackmore, M., Letourneau, P.C., 2006. J. Neurobiol. 66, 348 (Mar).
Blackmore, M.G., et al., 2010. Mol. Cell. Neurosci. 44, 43 (May).
Blackmore, M.G., et al., 2012. Proc. Natl. Acad. Sci. U. S. A. 109, 7517 (May 8).
Bomze, H.M., Bulsara, K.R., Iskandar, B.J., Caroni, P., Skene, J.H., 2001. Nat. Neurosci. 4, 38 (Jan).
Bonilla, I.E., Tanabe, K., Strittmatter, S.M., 2002. J. Neurosci. 22, 1303 (Feb 15).
Bregman, B.S., Kunkel-Bagden, E., McAtee, M., O'Neill, A., 1989. J. Comp. Neurol. 282, 355 (Apr 15).
Campbell, G., et al., 2005. Exp. Neurol. 192, 340 (Apr).
Case, L.C., Tessier-Lavigne, M., 2005. Curr. Biol. 15, R749 (Sep 20).
Chandran, V., et al., 2016. Neuron 89, 956 (Mar 2).
Chen, D.F., Jhaveri, S., Schneider, G.E., 1995. Proc. Natl. Acad. Sci. U. S. A. 92, 7287 (Aug 1).
Cho, Y., Cavalli, V., 2014. Curr. Opin. Neurobiol. 27, 118 (Aug).
Coffey, E.T., 2014. Nat. Rev. Neurosci. 15, 285 (May).
Dusart, I., Airaksinen, M.S., Sotelo, C., 1997. J. Neurosci. 17, 3710 (May 15).
Eva, R., Fawcett, J., 2014. Curr. Opin. Neurobiol. 27, 179 (Aug).
Fagoe, N.D., Attwell, C.L., Kouwenhoven, D., Verhaagen, J., Mason, M.R., 2015. Hum. Mol. Genet. 24, 6788 (Dec 1).
Finelli, M.J., Wong, J.K., Zou, H., 2013. J. Neurosci. 33, 19664 (Dec 11).
Fontana, X., et al., 2012. J. Cell Biol. 198, 127 (Jul 9).
Frank, C.L., et al., 2015. Nat. Neurosci. 18, 647 (May).
Frey, D., Laux, T., Xu, L., Schneider, C., Caroni, P., 2000. J. Cell Biol. 149, 1443 (Jun 26).
Gaub, P., et al., 2010. Cell Death Differ. 17, 1392 (Sep).
Geeven, G., et al., 2011. Nucleic Acids Res. 39, 5313 (Jul).
Gerhard, D.S., et al., 2004. Genome Res. 14, 2121 (Oct).
Goldberg, J.L., Klassen, M.P., Hua, Y., Barres, B.A., 2002. Science 296, 1860 (Jun 7).
Hai, T., Hartman, M.G., 2001. Gene 273, 1 (Jul 25).
Hobson, S.A., Vanderplank, P.A., Pope, R.J., Kerr, N.C., Wynick, D., 2013. J. Neurochem. 127, 199 (Oct).
Hunt, D., Raivich, G., Anderson, P.N., 2012. Front. Mol. Neurosci. 5, 7.
Jin, D., et al., 2015. Nat. Commun. 6, 8074.
Karimi-Abdolrezaee, S., Verge, V.M., Schreyer, D.J., 2002. Exp. Neurol. 176, 390 (Aug).
Koche, R.P., et al., 2011. Cell Stem Cell 8, 96 (Jan 7).
Langst, G., Manelyte, L., 2015. Genes (Basel) 6, 299.
Lee, K.K., Workman, J.L., 2007. Nat. Rev. Mol. Cell Biol. 8, 284 (Apr).
Lee, J.Y., et al., 2012. J. Neurochem. 121, 818 (Jun).
Lerch, J.K., Martinez-Ondaro, Y.R., Bixby, J.L., Lemmon, V.P., 2014. Mol. Cell. Neurosci. 59, 97 (Mar).
Li, S., et al., 2015. Sci. Report. 5, 16888.
Lin, S., Smith, G.M., 2015. Neural Regen. Res. 10, 1034 (Jul).
Lin, S., Nazif, K., Smith, A., Baas, P.W., Smith, G.M., 2015. J. Neurosci. Res. 93, 1215 (Aug).
Lv, L., et al., 2011. Brain Res. 1396, 60 (Jun 17).
Lv, L., Han, X., Sun, Y., Wang, X., Dong, Q., 2012. Exp. Neurol. 233, 783 (Feb).
Ma, T.C., Willis, D.E., 2015. Front. Mol. Neurosci. 8, 43.
Makwana, M., et al., 2010. J. Comp. Neurol. 518, 699 (Mar 1).
Mason, M.R., Lieberman, A.R., Anderson, P.N., 2003. Eur. J. Neurosci. 18, 789 (Aug).
Michaelevski, I., et al., 2010. Sci. Signal. 3, ra53.
Moore, D.L., et al., 2009. Science 326, 298 (Oct 9).
Nakagomi, S., Suzuki, Y., Namikawa, K., Kiryu-Seo, S., Kiyama, H., 2003. J. Neurosci. 23, 5187 (Jun 15).
Nemeth, A., Langst, G., 2004. Brief. Funct. Genomic. Proteomic. 2, 334 (Feb).
Pearson, A.G., et al., 2003. Brain Res. Mol. Brain Res. 120, 38 (Dec 12).
Plunet, W., Kwon, B.K., Tetzlaff, W., 2002. J. Neurosci. Res. 68, 1 (Apr 1).
Puttagunta, R., et al., 2014. Nat. Commun. 5, 3527.
Raivich, G., et al., 2004. Neuron 43, 57 (Jul 8).
Ruff, C.A., et al., 2012. J. Neurochem. 121, 607 (May).
Saijilafu, E., Hur, M., Zhou, F.Q., 2011. Nat. Commun. 2, 543.
Saul, K.E., Koke, J.R., Garcia, D.M., 2010. Comp. Biochem. Physiol. A Mol. Integr. Physiol. 155, 172 (Feb).
Seijffers, R., Mills, C.D., Woolf, C.J., 2007. J. Neurosci. 27, 7911 (Jul 25).
Shokouhi, B.N., et al., 2010. BMC Neurosci. 11, 13.
Simpson, M.T., et al., 2015. Mol. Cell. Neurosci. 68, 272 (Sep).
Sun, F., He, Z., 2010. Curr. Opin. Neurobiol. 20, 510 (Aug).
Sun, F., et al., 2011. Nature 480, 372 (Dec 15).
Tang, W., et al., 2009. J. Neurosci. 29, 8621 (Jul 8).
Tedeschi, A., 2011. Front. Mol. Neurosci. 4, 60.
Trakhtenberg, E.F., Goldberg, J.L., 2012. Front. Mol. Neurosci. 5, 24.
Tsujino, H., et al., 2000. Mol. Cell. Neurosci. 15, 170 (Feb).
van Kesteren, R.E., Mason, M.R., Macgillavry, H.D., Smit, A.B., Verhaagen, J., 2011. Front. Mol. Neurosci. 4, 46.
Vastenhouw, N.L., et al., 2010. Nature 464, 922 (Apr 8).
Wang, Z., Reynolds, A., Kirry, A., Nienhaus, C., Blackmore, M.G., 2015. J. Neurosci. 35, 3139 (Feb 18).
Williams, K.L., Rahimtula, M., Mearow, K.M., 2005. BMC Neurosci. 6, 24.
Yang, X.J., Seto, E., 2007. Oncogene 26, 5310 (Aug 13).
Yiu, G., He, Z., 2006. Nat. Rev. Neurosci. 7, 617 (Aug).
Zhang, Y., et al., 2005. Proc. Natl. Acad. Sci. U. S. A. 102, 14883 (Oct 11).
Zou, Y., et al., 2015. J. Neurosci. 35, 10429 (Jul 22).